JOURNAL OF MATERIALS SCIENCE 37 (2002) 2597–2606

Crystallization, microstructure development and dielectric behaviour of glass ceramics in the system $[SrO \cdot TiO_2]$-$[2SiO_2 \cdot B_2O_3]$-La_2O_3

O. P. THAKUR*, D. KUMAR‡, OM PARKASH
Department of Ceramic Engineering, Institute of Technology, Banaras Hindu University, Varanasi 221005, India
E-mail: omprakasht@hotmail.com

L. PANDEY
Department of Post-graduate Studies and Research in Physics, Rani Durgavati University, Jabalpur 482001, India

Various glasses in the system $(65 - x)[SrO \cdot TiO_2]$-$(35)[2SiO_2 \cdot B_2O_3]$-$(x)La_2O_3$, where $x = 1,5,10$ (wt%) were prepared by melting in alumina crucible (1375–1575 K). Heat treatment schedules were selected from DTA plots of respective glasses. X-ray diffraction studies of glass ceramic samples containing different concentrations of La_2O_3 revealed the formation of $Sr_2B_2O_5$, $Sr_3Ti_2O_7$ and TiO_2 (rutile) phases. The addition of La_2O_3 results in the development of well formed, elongated crystallites of different phases. Results of the dielectric behaviour demonstrate higher values of dielectric constant for some of the glass ceramic samples. This can be ascribed to the relaxation polarization at the crystal-glass interface due to conductivity differences between crystalline and glassy phases.
© *2002 Kluwer Academic Publishers*

1. Introduction

Soon after the pioneering work of Stookey [1] the controlled crystallization of glasses resulting in so called "glass ceramics" [2], considerable interest has developed in this field because of their interesting properties. Such glass ceramic specimens are free from pores in contrast to conventionally sintered ceramics. Glass ceramic bodies having intricate shapes and close tolerance in dimensions can be produced using commercial methods of glass production. This is an efficient way of producing uniform fine grains of crystalline phase in glassy matrix that is highly desirable. These features prompted several workers to develop glass ceramics containing ferroelectric phases such as, $BaTiO_3$ [3, 4], $PbTiO_3$ [5–7] and $NaNbO_3$ [8] etc.

Strontium titanate is a perovskite material with large dielectric constant and low dielectric loss. Over the last few years, efforts are also being made to precipitate $SrTiO_3$ phase in a glassy matrix and investigate corresponding dielectric and microstructure development [9–13]. Strontium titanate glass ceramic has been widely used in the field of cryogenics as capacitive temperature sensors [14] and has been applied for several technological applications where thermal stability of dielectric constant is required.

One study of the crystallization behaviour of strontium titanate aluminosilicate glass ceramics [15] shows that the $SrTiO_3$ phase precipitates along with several unwanted phases in a complex manner. The purity of starting raw materials and nucleation heat treatment play a significant role in the precipitation of strontium titanate in the glassy matrix [16]. Very little attention has been paid to the study of the crystallization behaviour of glass ceramics in this system. Recently we have investigated the crystallization and microstructural behaviour of strontium titanate borosilicate glass ceramic system without any additive [17] and with the addition of alkali oxide [12], CoO [13] and Bi_2O_3 [18]. It has been found that the addition of these oxides significantly affects crystallization, microstructure development and dielectric properties. Addition of alkali oxide results in the precipitation of $SrTiO_3$ as a major phase [12].

In the present paper we report the effect of La_2O_3 additions on the dielectric, crystallization and microstructure development of the borosilicate glass ceramic system.

2. Experimental procedure

Glasses were prepared from commercially available AR grade chemicals $SrCO_3$, TiO_2, SiO_2, H_3BO_3 and La_2O_3 of purity better than 99%. The ingredients in required proportions as shown in Table I were ground,

**Present Address:* Electroceramics Division, Solid State Physics Laboratory, Delhi 110054, India.
‡Author to whom all correspondence should be addressed.

TABLE I Glass compositions (wt%)

Glass no.	$(SrO \cdot TiO_2)$	$(2SiO_2 \cdot B_2O_3)$	La_2O_3	DTA peaks (°C) T_g	T_c
Base glass (Lo)	65	35	0	692	916
L1	64	35	1	687	867
L5	60	35	5	690	908
L10	55	35	10	696	913

mixed thoroughly and then melted in a high-grade alumina crucible at 1375–1575 K for 1 hour. The molten mass was stirred thoroughly to ensure good homogeneity of the melt. The molten mass was quenched by pouring it on to an aluminum mould and quickly pressing by aluminum plate to get specimens of uniform thickness. The samples were annealed at 700 K for 3 hrs. Glasses thus prepared were checked for their amorphous character by X-ray diffraction. Differential thermal analysis was carried out using a Model NETZSH, STA 409 before subjecting the samples to heat treatment for crystallization. Crystalline phases were identified by X-ray diffraction patterns using X-ray diffractometer (Model Rich-Seifert ID 3000) using Cu-Kα radiation. Samples were polished and etched using a solution of 2%HF + 5% HCl for 20–30 seconds. Etched samples were coated with Au-Pd alloy using a vapor deposition technique. Micrographs of these etched samples were recorded using a scanning electron microscope (Model Stereoscan 250MK III, Cambridge Instruments Ltd. UK). For the electrical measurements, silver electrodes were deposited on both sides of the sample and fired at 973 K for 5 minutes to make good electrical contacts. Dielectric measurements were carried out with the help of an Impedance Analyzer (Model HP 4192A LF) in the frequency range 100 Hz to 1 MHz at different temperatures.

3. Results and discussion

3.1. DTA study

Compositions of the base glass [17] and glasses containing different fractions of La_2O_3 are given in Table I. Fig. 1 shows the DTA patterns for glasses L1, L5 and L10 and base glass for comparison. Glass transition temperatures, T_g, and onsets of crystallization for these glasses were observed at around 690°C and 820°C respectively. An exothermic peak appearing at 916°C for the base glass corresponds to the crystallization temperature. A single exothermic peak was observed for these glasses similar to the base glass. Addition of 1 wt% La_2O_3 lowers the exothermic peak to 867°C. However, with further addition of La_2O_3 in the base glass (glass L5 and L10), crystallization temperature again starts shifting towards higher temperature. The exothermic peak for the glass L5 and L10 appears around 908°C and 913°C respectively. It can also be seen that the width of exothermic peak increases with increasing La_2O_3 concentration. This widening may be attributed to the slowing down of crystallization process with increasing concentration of La_2O_3. From X-ray diffraction analysis, it has been confirmed that the exothermic peak in DTA plot corresponds to the crystallization of

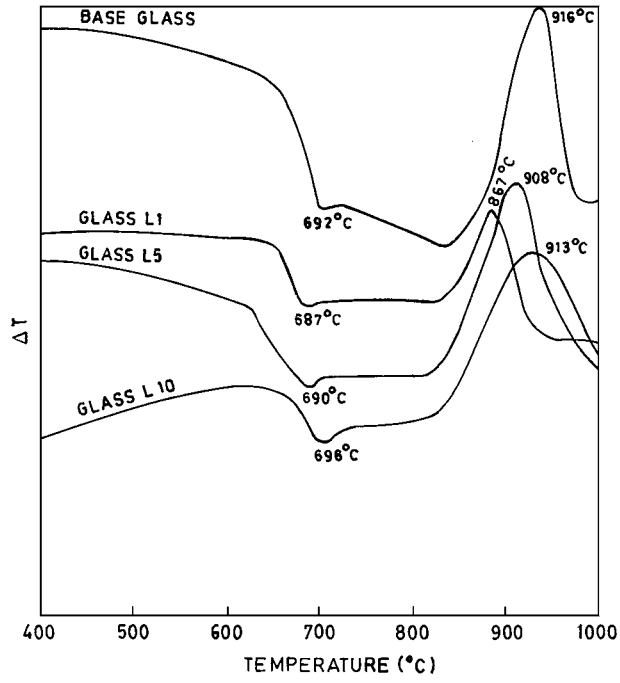

Figure 1 DTA pattern for glass (a) base glass, (b) L1, (c) L5 and (d) L10.

$Sr_2B_2O_5$, $Sr_3Ti_2O_7$ and TiO_2 (rutile) phases. It is evident that increasing La_2O_3 additions from 0 to 1% decrease the crystallization temperature for the glass whilst increases of 5 and 10% have little apparent effect on the crystallization temperature of the base glass.

3.2. Crystallization behaviour

Table II lists the heat treatment temperatures and crystalline phase constitution of various glass ceramic samples along with their nomenclature. XRD patterns for glass L1 crystallized at 900°C, 950°C and 1000°C are shown in Fig. 2. When glass L1 was subjected to heat treatment at 820°C (onset of crystallization) for 3 hrs, the resulting glass ceramic consisted of $Sr_2B_2O_5$, $Sr_3Ti_2O_7$ and some unidentified phases which have not been marked in XRD patterns. When the crystallization

TABLE II Heat treatment schedules and crystalline phase constituents

Glass no.	Glass ceramic no.	Heating rate (°C/min)	Heating time (hr)	Temperature (°C)	Crystalline phases
Lo	LoA	5	3	800	SB,ST,R
	LoB	5	3	860	SB,ST
	LoC	5	3	900	SB,ST,R
	LoD	5	3	950	SB,R,ST
L1	L1A	5	3	800	SB,ST
	L1B	5	3	900	SB,ST,R
	L1C	5	3	950	SB,ST,R
	L1D	2	6	1000	Rmax, SB,ST
L5	L5A	5	3	800	SB,ST
	L5B	5	1	860	SB,ST
	L5C	5	3	900	SB,ST,R
	L5D	5	3	950	SB,ST,R
	L5E	5	3	1000	SB,ST,R
L10	L10A	5	3	860	SB,ST,R
	L!0B	5	3	900	SB,ST,R
	L10C	5	3	950	SB,ST,R
	L10D	5	3	1000	SB,R,ST

Note: SB = $Sr_2B_2O_5$, ST = $Sr_3Ti_2O_7$ and R = TiO_2 (rutile) etc.

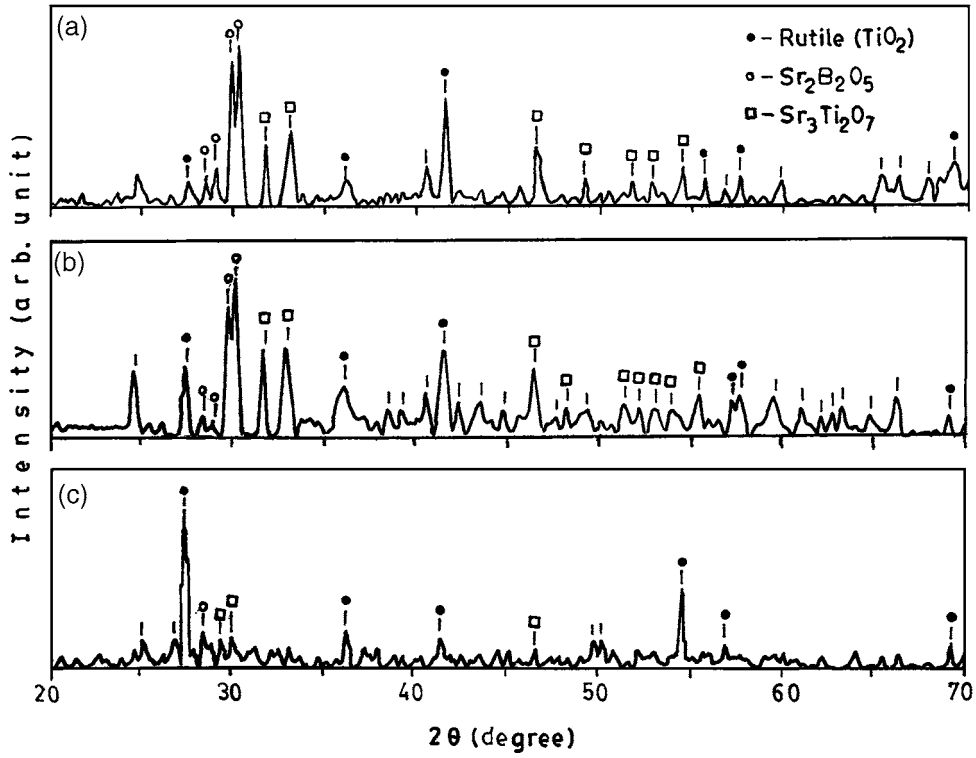

Figure 2 XRD patterns for glass L1 crystallized at (a) 900°C/3 hrs, (b) 950°C/3 hrs and (c) 1000°C/6 hrs.

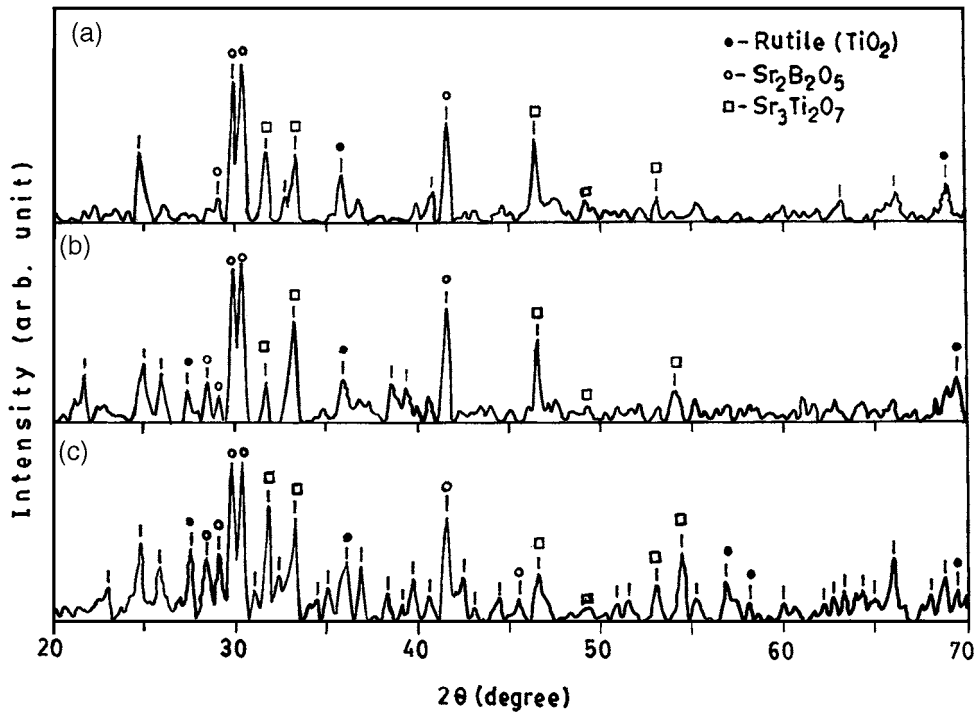

Figure 3 XRD patterns for glass L5 crystallized at (a) 900°C/3 hrs, (b) 950°C/3 hrs and (c) 1000°C/3 hrs.

temperature was increased to 900°C for 3 hrs, TiO_2 (rutile) phase started precipitating together with $Sr_2B_2O_5$ and $Sr_3Ti_2O_7$ phases. Intensities of XRD reflections for the rutile phase increase with increasing crystallization temperature. At 1000°C, TiO_2 (rutile) phase appears as the primary constituent while other phases such as $Sr_2B_2O_5$, $Sr_3Ti_2O_7$ appear as secondary ones.

X-ray diffraction pattern for glass L5, heat treated at 900°C, is shown in Fig. 3a. The pattern shows the presence of $Sr_2B_2O_5$, $Sr_3Ti_2O_7$ and unidentified phases. The unidentified phases are not marked in XRD patterns. As the crystallization temperature raised to 950°C, the intensity of rutile phase increases (Fig. 3b). XRD pattern of L5 crystallized at 1000°C (Fig. 3c) shows more intense reflections of $Sr_3Ti_2O_7$ along with $Sr_2B_2O_5$ and TiO_2 (rutile) phases.

The glass ceramic derived from glass L10 by heat treatment at 900°C shows the presence of $Sr_2B_2O_5$ and $Sr_3Ti_2O_7$ phases (Fig. 4a). A small amount of the rutile phase was also observed for this heat treatment schedule

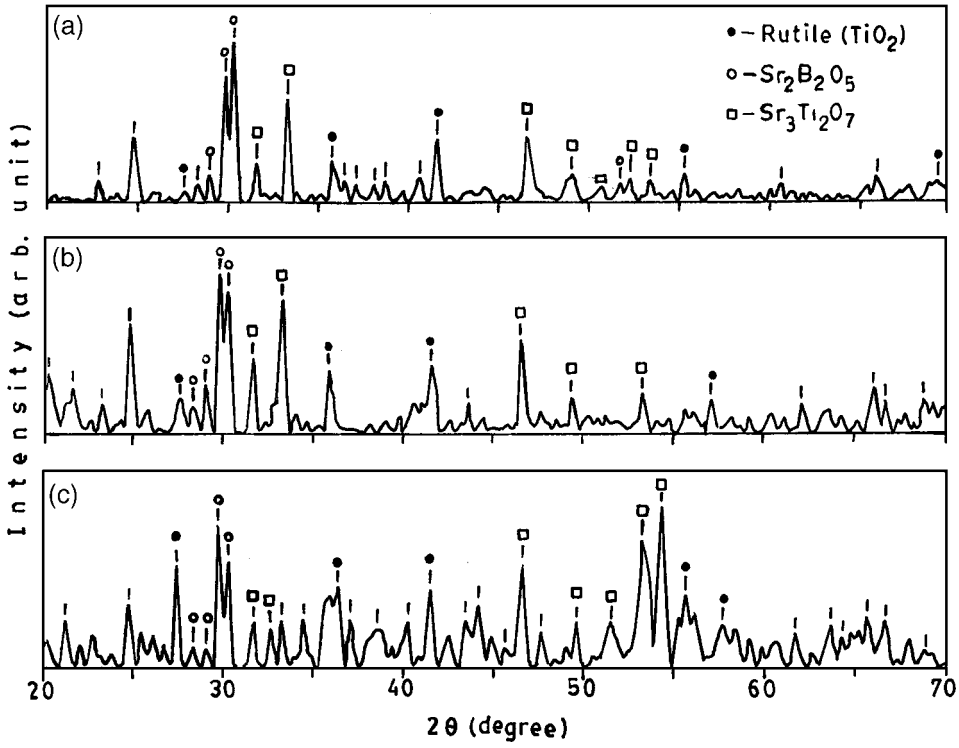

Figure 4 XRD patterns for glass L10 crystallized at (a) 900°C/3 hrs, (b) 950°C/3 hrs and (c) 1000°C/3 hrs.

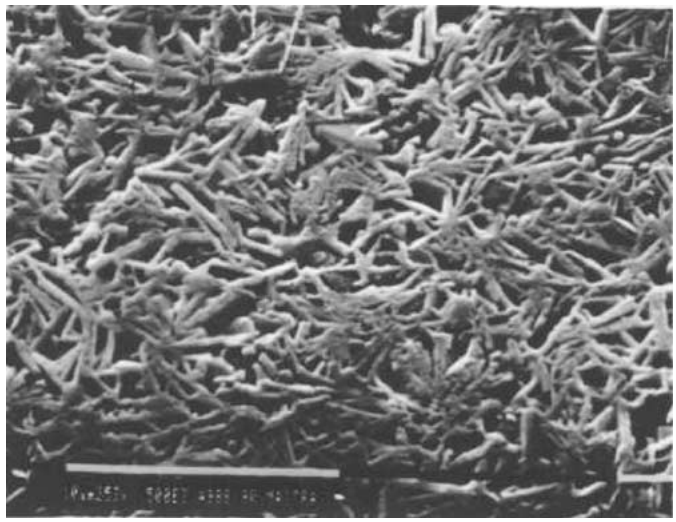

(a)

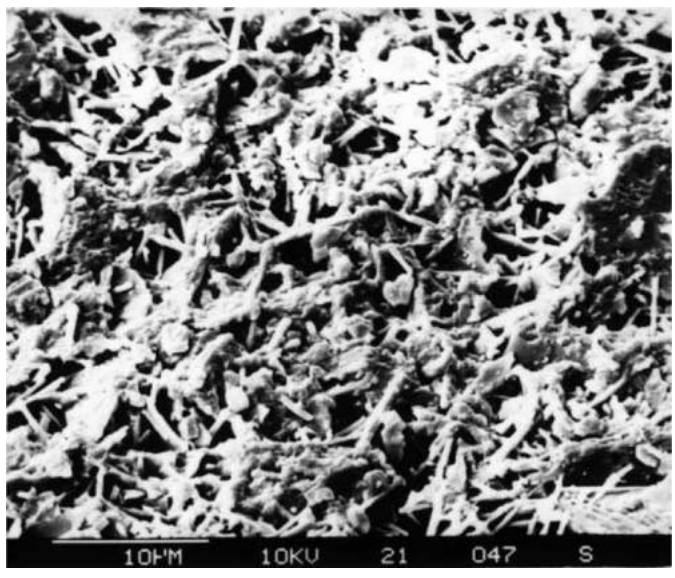

(b)

Figure 5 Scanning electron micrographs of base glass ceramics crystallized at (a) 900°C/3 hrs and (b) 950°C/3 hrs.

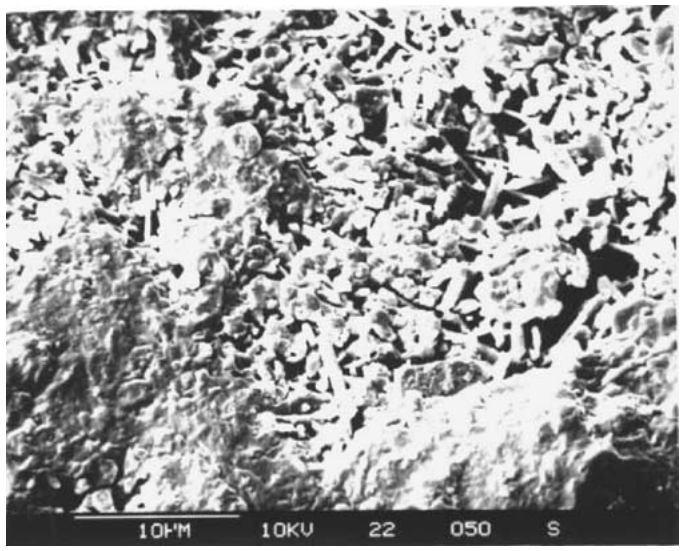

(a)

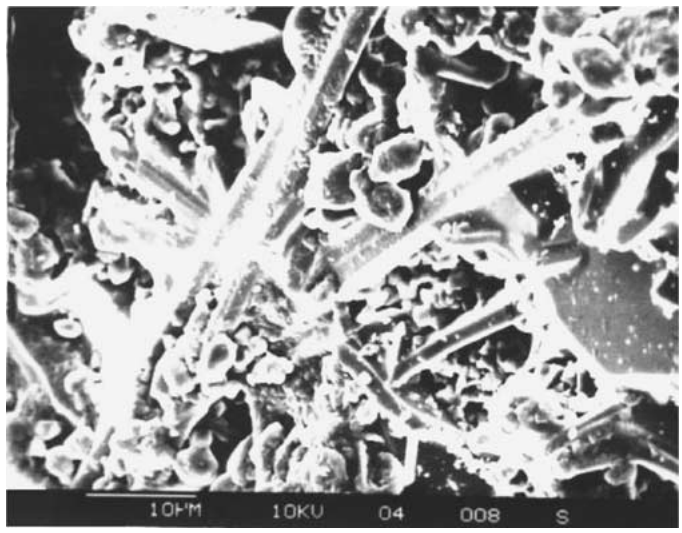

(b)

Figure 6 Scanning electron micrographs for glass L1 crystallized at (a) 950°C/3 hrs and (b) 1000°C/6 hrs.

which increases further with increasing temperature as shown in Fig. 4b. For this heat treatment the intensities of $Sr_2B_2O_5$ and $Sr_3Ti_2O_7$ reflections are almost comparable and high. The intensities of XRD reflections for the $Sr_3Ti_2O_7$ phase seem to increase up to a crystallization temperature of 950°C. On further increasing the crystallization temperature to 1000°C, the intensities corresponding to $Sr_3Ti_2O_7$ decrease. Fig. 4c shows the X-ray diffraction pattern of glass ceramic L10 crystallized at 1000°C for 3 hrs.

From the above crystallization study, it may be inferred that the heat treatment temperature selected from left half region of DTA exothermic peak reveals the precipitation of $Sr_2B_2O_5$ and $Sr_3Ti_2O_7$ phases while the heat treatment temperature from right half of DTA exothermic peak promotes the crystallization of TiO_2 (rutile) phase. At lower crystallization temperatures $Sr_2B_2O_5$, $Sr_3Ti_2O_7$ phases precipitate at faster rate while at higher temperatures, the crystallization of rutile phase becomes more rapid. The high concentration of La_2O_3 in the base glass (glass L10) at 950°C favours the crystallization of the $Sr_3Ti_2O_7$ phase. This may be inferred from the fact that the XRD peak intensity of $Sr_2B_2O_5$ and $Sr_3Ti_2O_7$ seems to be comparable at 950°C heat treatment. At 1000°C, the corresponding XRD peak of $Sr_3Ti_2O_7$ decreases while the intensity of TiO_2 peak increases.

3.3. Microstructure

A micrograph for the base glass heat treated at 900°C for 3 hrs (Fig. 5a) reveals crystallites of $Sr_2B_2O_5$, $Sr_3Ti_2O_7$ and TiO_2 (rutile) phases interconnected with each other. As the crystallization temperature is further raised to 950°C for 3 hrs (Fig. 5b), there is no major change observed in the morphology of the glass ceramic sample except that a little growth occurred in crystallites. The SEM micrograph of glass ceramic specimen L1C (Fig. 6a) depicts the distribution of $Sr_2B_2O_5$, $Sr_3Ti_2O_7$ and TiO_2 (rutile) phases. Fine crystallites of TiO_2 (rutile) and large crystallites of $Sr_2B_2O_5$ were observed. As the crystallization temperature is increased to 1000°C (Fig. 6b), further growth of $Sr_2B_2O_5$ crystallites (acicular type) was observed. The gap between borate crystallites is filled up by spherulitic crystals of $Sr_3Ti_2O_7$ phase. The SEM micrograph shown in Fig. 7a for glass ceramic L5 crystallized at 860°C for 1 hr shows

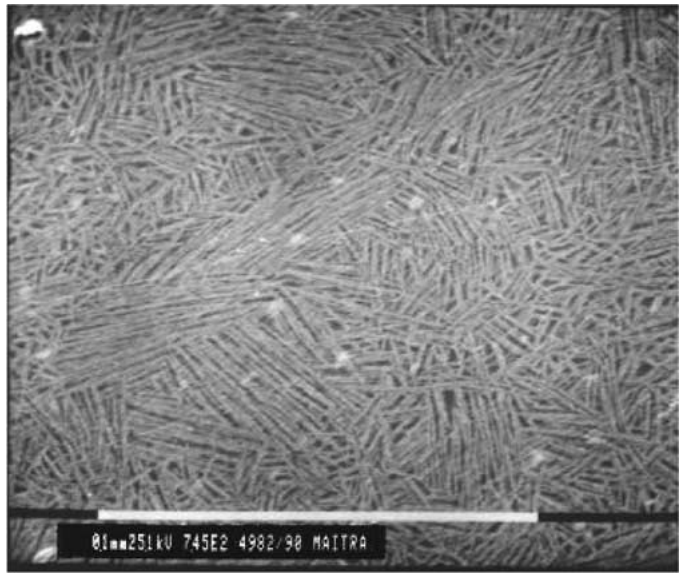

(a)

(b)

Figure 7 Scanning electron micrographs for glass L5 crystallized at (a) 860°C/1 hr and (b) 900°C/3 hrs.

fine grains of the $Sr_2B_2O_5$ phase. As the crystallization temperature is increased (Fig. 7b), the grain size of the $Sr_2B_2O_5$ phase increases. This is accompanied by the crystallization of the $Sr_3Ti_2O_7$ phase. Thus, with increasing concentration of lanthanum oxide (5 wt% La_2O_3) resulting glass ceramics exhibit a dense, uniform and fine crystalline microstructure. Some black spots visible in this micrograph for unetched samples represent an unidentified phase which disappears during etching along with the glassy regions.

Fig. 8 shows scanning electron micrographs of glass ceramic samples L10, crystallized under different heat treatment schedules. Fig. 8a shows uniformly distributed and well inter-linked crystallites of the $Sr_2B_2O_5$ phase in glass ceramic sample L10 crystallized at 860°C for 3 hrs. Very fine grains of $Sr_3Ti_2O_7$ were seen along the edges of the borate phase and seem to grow with increasing crystallization temperature and longer holding times (Fig. 8b and c). Growth of the borate phase was also noticed. Grain diameters of the borate phase fall in the range 1–2 μm whereas it is in the sub-micron range for $Sr_3Ti_2O_7$ phase. Spherical grains present in the background of the needle (rutile phase) and plate like ($Sr_2B_2O_5$) morphology represent $Sr_3Ti_2O_7$ phase. It is observed that the space among $Sr_2B_2O_5$ crystallites was filled up by $Sr_3Ti_2O_7$ granules. In other words, it may be inferred that the higher La_2O_3 content in base glass supports the precipitation of $Sr_3Ti_2O_7$ phase that meets in agreement with XRD results.

3.4. Dielectric behaviour

Fig. 9a and b shows the variation of dissipation factor tan(δ) and dielectric constant (ε') with temperature for glass ceramic specimen L1C. Dielectric constant increases with temperature and decreases with increasing frequency. The magnitude of ε' and tan(δ) falls in the range 200–1000 and 0.15–0.35 respectively. As shown in Fig. 9c, maxima are observed in the variation of tan(δ)

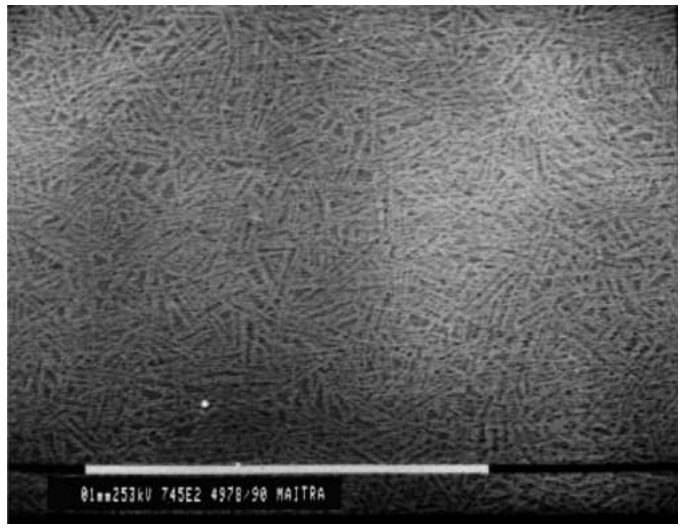

(a)

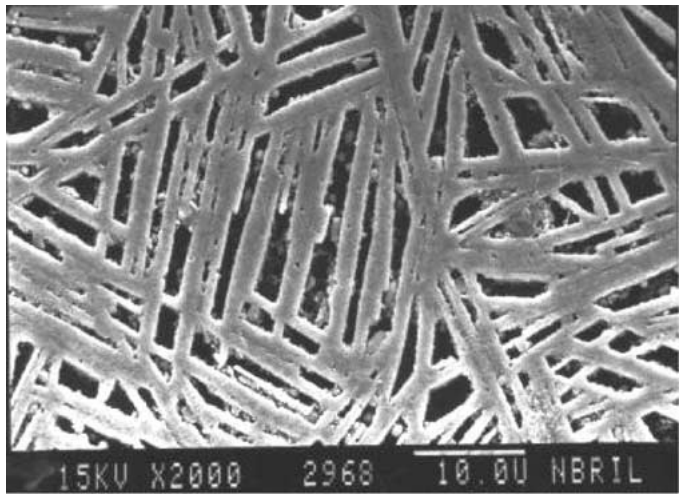

(b)

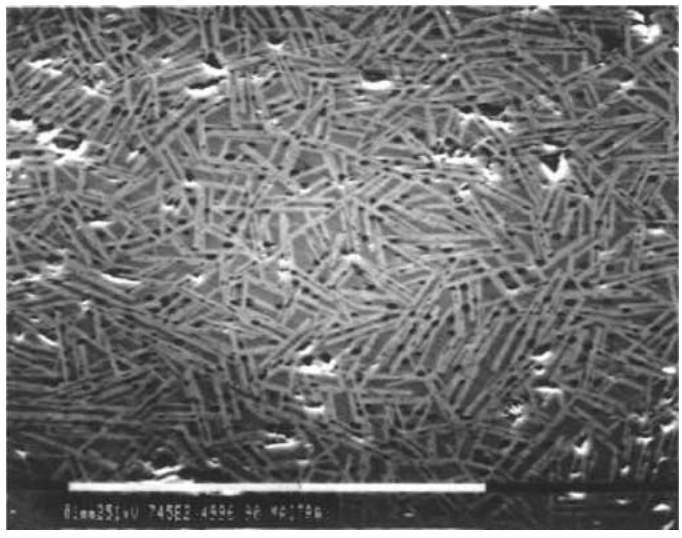

(c)

Figure 8 Scanning electron micrographs for glass L10 crystallized at (a) 860°C/3 hrs, (b) 900°C/3 hrs and (c) 950°C/3 hrs.

with respect to frequency. The dissipation peak width decreases with increasing temperature and the peak frequency shifts to higher values with increasing temperature. This may be ascribed to relaxation of space charge polarization. The different trend of variation in dissipation factor-temperature plot (Fig. 9a) above and below the frequency of maxima (100 kHz) can be understood by observation of tan(δ)- log(f) plots (Fig. 9c). At low frequency dissipation factor decreases with temperature while it shows reverse trend at higher frequency side of maxima. The activation energy calculated from the logarithm of peak frequency vs T^{-1} plot was found to be 0.24×10^{-19} J for this glass ceramic specimen L1C.

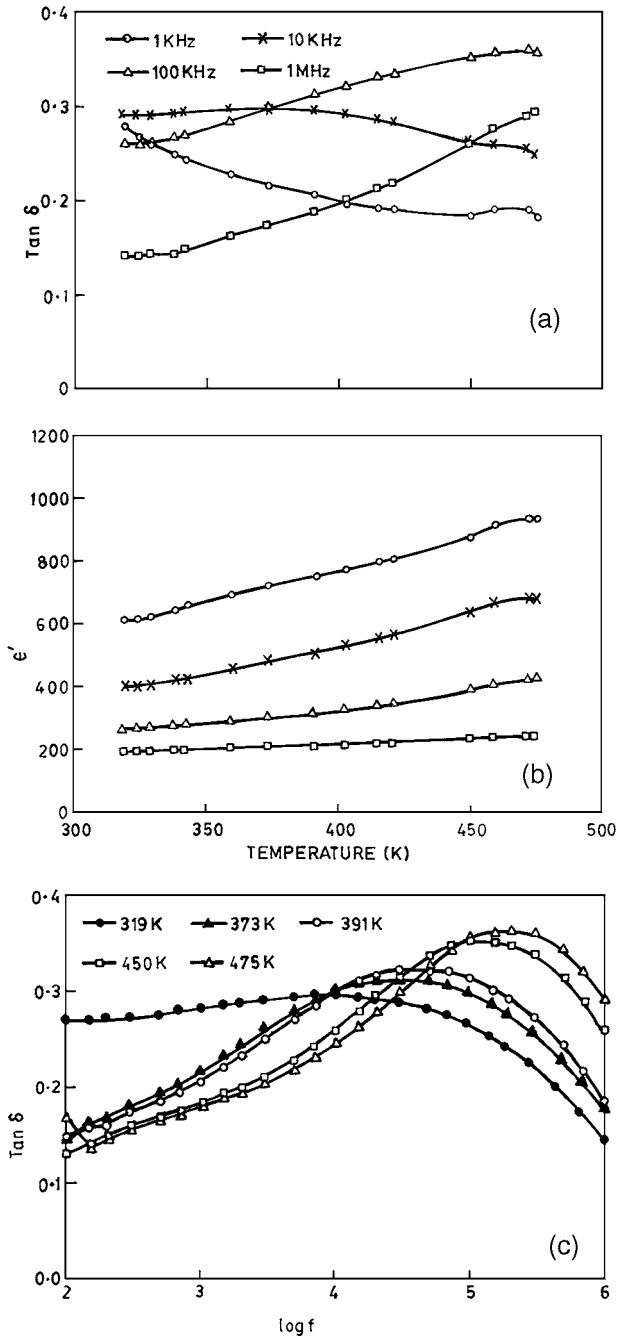

Figure 9 Temperature variation of (a) dissipation factor, tan(δ), (b) dielectric constant (ε') and (c) frequency variation of dissipation factor for glass L1 crystallized at 950°C for 3 hrs.

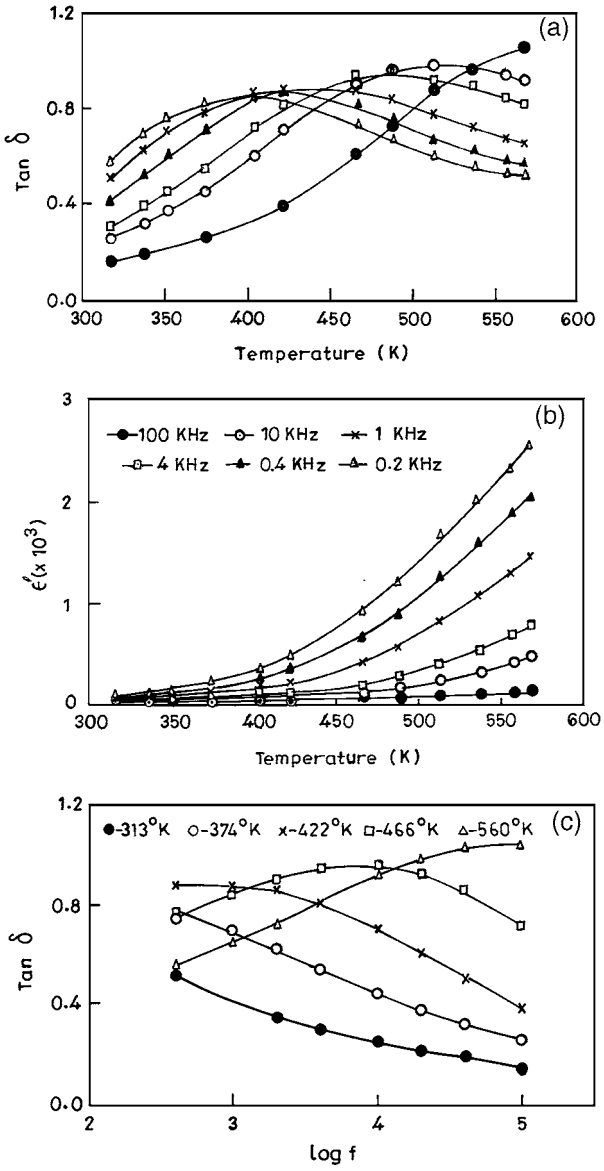

Figure 10 Temperature variation of (a) dissipation factor, tan(δ), (b) dielectric constant (ε') and (c) frequency variation of dissipation factor for glass L5 crystallized at 900°C for 3 hrs.

The dielectric constant and dissipation factor for glass L5 crystallized at 860°C for 1 hr, gradually changes with temperature (Fig. 10a and b). Both ε' and tan(δ) show more dispersion in low frequency range which becomes less appreciable at higher frequencies. The values of ε' and tan(δ) for this glass ceramic samples are small and in the range of 30–45, 0.01–0.3 respectively. The increase in dielectric constant (20–3000) and dissipation factor (0.1–1.0) of glass ceramic L5C (Fig. 10) seems to be due to interfacial or space charge polarization, which is thought to be arising from the difference between the conductivity of various phases. Broad relaxation peaks were observed for the variation of dissipation factor with respect to temperature and frequency that shows the relaxation character of the losses. The broad peaks in these plots show the presence of distribution of relaxation times. The logarithmic plot of the peak frequency against reciprocal temperature is having average activation energy of 1.22×10^{-19} J.

The dielectric constant and dissipation factor of glass ceramic L10 crystallized at 860°C for 3 hrs, both increase very slowly with temperature and show high dispersion in the lower frequency region. This trend may be attributed to the very small amount of crystalline phase present in the glassy matrix. A further increase in crystallization temperature (900°C for 1 hr) enhances the value of dielectric constant, which is in the range of 20–500. The value of ε' varies very little up to a particular temperature, after which it levels off. A similar trend was also observed for the temperature variation of tan(δ). The value of tan(δ) is in the range 0.05–1.25 for this glass ceramic sample which seems to be high and caused by space charge polarization. Both ε' and tan(δ) show little dispersion below the particular temperature after which it becomes quite pronounced. When the holding time at 900°C is increased to 3 hrs

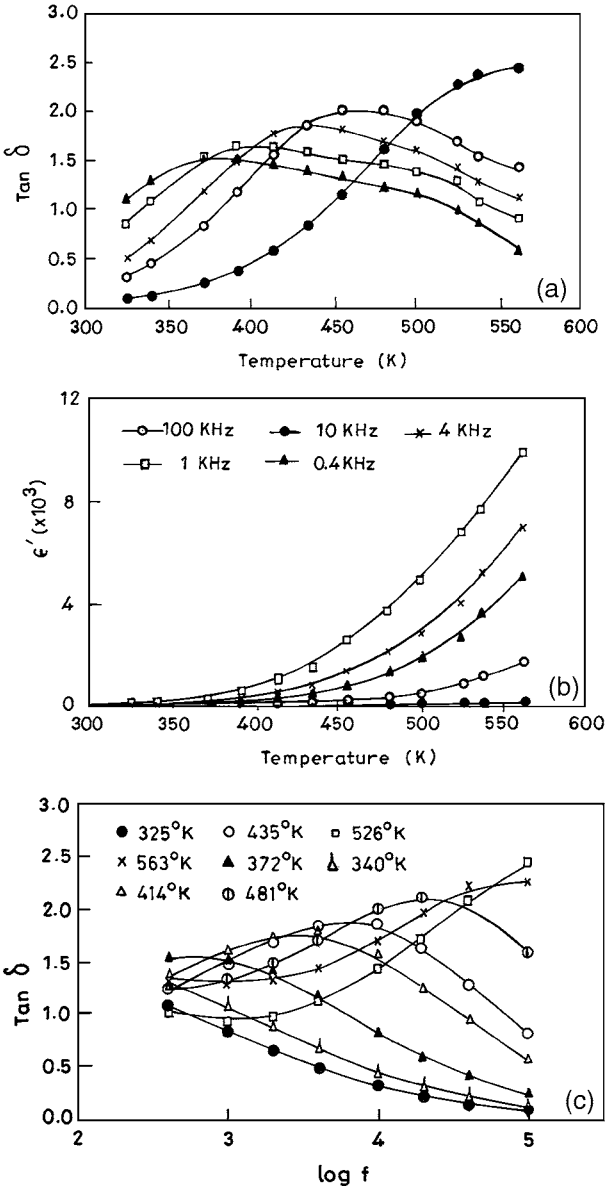

Figure 11 Temperature variation of (a) dissipation factor, tan(δ), (b) dielectric constant (ε') and (c) frequency variation of dissipation factor for glass L10 crystallized at 900°C 11 for 3 hrs.

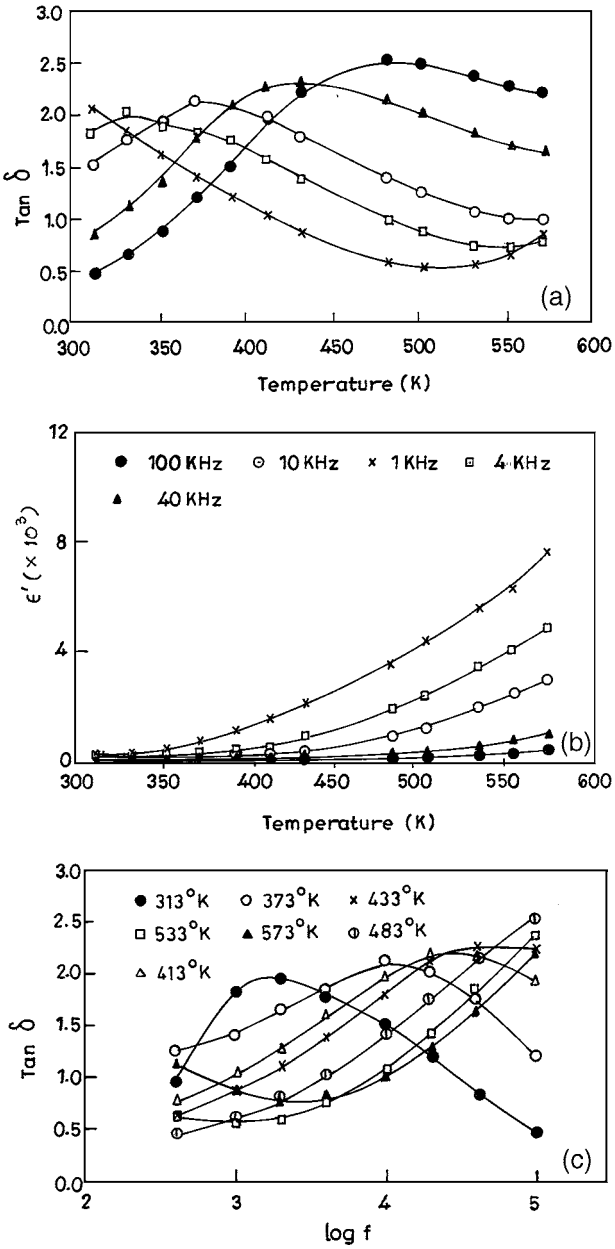

Figure 12 Temperature variation of (a) dissipation factor, tan(δ), (b) dielectric constant (ε') and (c) frequency variation of dissipation factor for glass L10 crystallized at 950°C for 3 hrs.

(glass ceramic L10B), a very high value of dielectric constant (100–12000) was observed (Fig. 11) owing to space charge polarization [15]. The temperature and frequency dependence of tan(δ) (Fig. 11) show relaxor behaviour. The activation energy obtained for this glass ceramic sample is 0.93×10^{-19} J. The higher value of tan(δ) (0.05–2.5) may be due to high conduction loss in the residual glassy phase. A similar behaviour of the dielectric constant was also observed for the glass ceramic sample L10C as shown in Fig. 12. The activation energy for this glass ceramic is 0.50×10^{-19} J.

From the above study, it is thought that the presence of La^{3+} ions may reduce some of the Ti^{4+} ions into Ti^{3+} ions. Consequently, the electrical conductivity of glass, crystallites or glass-crystal interface region or combination of these may increase due to electron hopping between Ti^{3+} and Ti^{4+} ions. Reduction of Ti^{4+} ions may also arise due to several factors like, higher crystallization temperature, period of heat treatment, concentration of additives and processing schedules etc.

4. Conclusions

(i) The heat treatment of glass L1 containing 1 wt% La_2O_3 shows the formation of $Sr_2B_2O_5$ and $Sr_3Ti_2O_7$ phases at low temperatures. Rutile (TiO_2) phase appears at higher temperature heat treatment (950°C) and crystallizes in major amount at 1000°C.

(ii) In case of glass L5 (5 wt% La_2O_3), rutile (TiO_2) phase starts emerging from 950°C onwards as a secondary phase while $Sr_3Ti_2O_7$ appears as primary phase at higher temperature (1000°C) treatments.

(iii) For glass L10 (10 wt%La_2O_3), the XRD peak intensity corresponding to $Sr_3Ti_2O_7$ phase increases up to 950°C and then starts decreasing at higher temperature (1000°C) treatments. This may be caused by the decomposition of $Sr_3Ti_2O_7$ at high temperature that in turn forms TiO_2 (rutile) phase. The XRD peak intensity of TiO_2 (rutile) phase increases at 1000°C.

(iv) From the crystallization study of this system, it has been observed that the $Sr_2B_2O_5$ and $Sr_3Ti_2O_7$

phases precipitate quite faster at low temperature treatments while at higher temperatures, the crystallization of TiO_2 (rutile) phase becomes more rapid.

(v) The addition of La_2O_3 in strontium titanate borosilicate glass ceramic system results in elongated, interlinked and well-formed crystallites of $Sr_2B_2O_5$, $Sr_3Ti_2O_7$ and TiO_2 phases.

(vi) Higher values of dielectric constant were observed for this glass ceramic system that may be attributed to the conductivity difference between different crystallites and glassy matrix.

Acknowledgements

We are highly grateful to Late Jain Prakash who had provided us some samples for the present paper. One of the authors (OPT) is indebted to the Department of Atomic Energy, Trombay for awarding Dr. K.S. Krishnan Research fellowship. Partial financial support from UGC and CSIR, New Delhi is gratefully acknowledged.

References

1. S. D. STOOKEY, Glasstech. Ber. 32K (Fifth International Congress on glass, Verlag der Deutschen Glasstechnischen Gesellschaft, Frankfurt am Main) (1959) p. 574.
2. P. W. MC MILLAN, in "Glass Ceramics" (Academic Press, London, 1979).
3. A. HERCZOG, *J. Amer. Ceram. Soc.* **47** (1964) 107.
4. *Idem., ibid.* **67** (1984) 484.
5. D. G. GROSSMAN and J. O. ISARD, *ibid.* **52** (1969a) 230.
6. *Idem., J. Mater. Sci.* **4** (1969b) 1059.
7. S. M. LYNCH and J. E. SHELBY, *J. Amer. Ceram. Soc.* **67** (1984) 424.
8. M. M. LAYTON and A. HERCZOG, *ibid.* **50** (1967) 369.
9. S. L. SWARTZ, A. S. BHALLA, L. E. CROSS and W. N. LAWLESS, *J. Mater. Sci.* **23** (1988) 4004.
10. S. L. SWARTZ, E. BREVAL, C. A. RANDALL and B. H. FOX, *ibid.* **23** (1988) 3997.
11. O. P. THAKUR, D. KUMAR, O. PARKASH and L. PANDEY, *Mater. Lett.* **23** (1995) 253.
12. *Idem.*, *Bull. Mater. Sci.* **19** (1996) 393.
13. W. N. LAWLESS, *Rev. Sci. Instrum.* **42** (1972) 561.
14. S. L. SWARTZ and A. S. BHALLA, *Mat. Res. Bull.* **21** (1986) 1417.
15. S. L. SWARTZ, Ph. D. Thesis, The Pennsylvania State University, USA (1985).
16. S. L. SWARTZ, E. BREVAL and A. S. BHALLA, *Am. Ceram. Soc. Bull.* **67** (1988) 763.
17. O. P. THAKUR, D. KUMAR, O. PARKASH and L. PANDEY, *Bull. Mater. Sci.* **18** (1995) 577.
18. *Idem.*, *Indian J. Phys.* **71A** (1997) 161.

Received 18 July 1997
and accepted 30 January 2002